

N62-10644

NASA TN D-1160

NASA TN D-1160



TECHNICAL NOTE

D-1160

FLIGHT-DETERMINED AERODYNAMIC-NOISE ENVIRONMENT OF AN
AIRPLANE NOSE CONE UP TO A MACH NUMBER OF 2

By Norman J. McLeod

Flight Research Center
Edwards, Calif.

NATIONAL AERONAUTICS AND SPACE ADMINISTRATION
WASHINGTON

March 1962

Reproduced by
NATIONAL TECHNICAL
INFORMATION SERVICE
Springfield, Va. 22151

NATIONAL AERONAUTICS AND SPACE ADMINISTRATION

TECHNICAL NOTE D-1160

FLIGHT-DETERMINED AERODYNAMIC-NOISE ENVIRONMENT OF AN
AIRPLANE NOSE CONE UP TO A MACH NUMBER OF 2

By Norman J. McLeod

SUMMARY

The aerodynamic-noise environment of a Fiberglas nose cone for a fighter-type airplane was measured over a Mach number range from 0.8 to 2. The measurements were obtained at altitudes of about 26,000 feet and 40,000 feet for a dynamic-pressure range of approximately 200 lb/sq ft to 1,000 lb/sq ft.

The data showed that the aerodynamic-noise level on the surface of the cone increased with free-stream dynamic pressure. The average noise pressure varied from approximately 0.001 of the lower dynamic pressures to approximately 0.0005 of the higher dynamic pressures. The noise level in the octave bands below 2,400 cycles per second showed large deviations from the mean, which would cause serious error in structural-fatigue tests when such tests are based on the average level. Variations in angle of attack of from 1° to 5° had negligible effect on the noise levels; however, at an altitude of 40,000 feet and an angle of attack of approximately 0°, intermittent increases in noise levels were measured.

INTRODUCTION

Noise has become an important consideration in the design of airplanes, inasmuch as it may cause structural or equipment failure and human discomfort. The three sources of aircraft noise are engine noise, internal equipment, and aerodynamic noise. Engine noise has been investigated theoretically and experimentally, and considerable data are available. Noise due to internal equipment varies to such a large extent that no general theoretical or experimental approach is possible. The contribution of aerodynamic noise to the noise environment of airplanes has not been fully determined, although many studies of aerodynamic noise have been made.

H
1
6
0

Theoretical approaches to aerodynamic noise presented in references 1 and 2 are for the aerodynamic noise propagated away from a body. The relationship between the noise propagated away from a body and the noise environment of a body is not fully understood. Aerodynamic noise developed in subsonic pipe flow was investigated in the study of reference 3. Measurements of aircraft noise environment in flight are presented in references 4 and 5. Reference 4 presents measurements of aerodynamic noise on an airplane wing at subsonic speeds, and reference 5 presents measurements of aerodynamic noise for the fuselage of one airplane at subsonic speeds and limited internal-noise measurements for the fuselage of another airplane at supersonic speeds.

The NASA Flight Research Center, Edwards, Calif., is conducting a program to determine aerodynamic noise at supersonic speeds utilizing a fighter-type aircraft equipped with a Fiberglas nose cone. This paper presents the results of measurements made on the nose cone as an aid in determining the aerodynamic-noise environment in this area of an aircraft.

H
1
6
0

SYMBOLS

h_p	pressure altitude, ft
M	Mach number
q	free-stream dynamic pressure, lb/sq ft
t	time, sec
α	nose-cone angle of attack, deg

DESCRIPTION OF NOSE CONE

The nose cone used in this investigation is a production Fiberglas cone with walls approximately 5/16 inch thick. The cone was modified by replacing the standard nose-boom mount with an aluminum insert and turning the first 22 inches to a true conical surface, with an included angle of 24.5°. The cone was faired smoothly to the mounting ring and hand-polished so that it had a surface roughness of 7 to 9 microns. A vented aluminum mounting ring was used to attach the Fiberglas cone to the test airplane. The vent had an area of 5 square inches. Figure 1 shows a sketch of the nose cone and mounting ring, and illustrates the deviation from a true cone of 24.5°.

INSTRUMENTATION AND DATA REDUCTION

Instrumentation

Three microphones were used in this investigation. The positions at which measurements were made are shown in figures 2(a) and 2(b). Microphone A, an Altec Lansing 21BR-180-7 microphone equipped with a sintered bronze wind screen, was mounted flush with the outside surface of the cone at station 55 to measure the pressure fluctuations in the boundary layer. Microphone B, a Western Electric 640AA microphone, was initially mounted facing forward at station 10 to measure the internal-noise level due to a laminar boundary layer. The microphone mount at station 10 divided the cone into two acoustic sections. Microphone B was also mounted, for part of the tests, at station 55 in an acoustic isolation chamber so constructed that measurements of noise transmitted through the wall of the cone could be made. The acoustic isolation chamber was mounted symmetrically in the cone with respect to microphone A. Microphone C, a Western Electric 640AA microphone, was mounted facing forward at station 55 to measure the internal-noise level due to a turbulent boundary layer.

The electronic components used with microphone A were an Altec Lansing 165A base and 526A power supply. Microphone B was equipped with a Western Electro-Acoustic 100-E preamplifier and power supply, and Microphone C was equipped with a Western Electric RA-1095 preamplifier and a NASA power supply. Accelerometers were mounted on all microphones at station 55 to show that no erroneous microphone signals were caused by structural accelerations. The microphone and accelerometer data were recorded on magnetic tape.

The boundary-layer microphone (A) was mounted rigidly to the cone. All other microphone mounts were vibration-isolation mounts operating on the same principles as the mounts used in reference 5.

A boundary-layer rake was mounted at station 55 for two flights, in place of microphone A, to determine the approximate boundary-layer thickness.

Standard NASA film-recording instruments were used to record air-speed, altitude, aircraft accelerations, and the boundary-layer-rake pressures. All instrumentation was correlated with a common timer.

Data Reduction

The data were played back and oscillograph records of the overall noise levels and octave-band levels were obtained. A General Radio 1550-A Octave-Band Noise Analyzer was used to obtain the octave-band

analysis, and a Panoramic Sonic Spectrum Analyzer was used to monitor the data and determine that the noise in the octave bands was continuous and that no discrete frequencies were present.

The write-out system had a response of 67 percent of the change in noise level in decibels in 0.075 second, and 100 percent in 0.15 second. The system was 69 percent critically damped with an overshoot of 4.7 percent of the change in noise level in decibels. Time histories of the noise levels indicated that overshoot was not a problem in the write-out system.

The maximum level in decibels at a given free-stream dynamic pressure was determined by fairing the maximum levels of the recorded data over a dynamic-pressure range of approximately ± 10 lb/sq ft. The minimum noise level was determined in the same manner. The mean noise level at a given airplane dynamic pressure was obtained by averaging the maximum and the minimum faired values. This method of data reduction was used because the data had variations as great as 15 decibels in less than 1 second. Integration of typical data indicated that the faired average values were within ± 0.5 decibel of the integrated values.

H
1
6
0

Calibration

Preflight and postflight acoustic calibrations at 1,000 cps were used to determine the noise level of the data. Since microphones do not have a flat frequency response, laboratory calibrations were obtained. A parallel-incidence calibration of microphone A and a reciprocity calibration of microphone C were supplied by the National Bureau of Standards. A pressure calibration was supplied by the Western Electro-Acoustic Laboratory, Inc., for microphone B. The microphone calibrations are shown in figures 3(a) to 3(c). The calibrations are presented as the variation in decibels from the response at 1,000 cps for a constant calibration-input level from 50 cps to 10,000 cps. The response at 1,000 cps is plotted as the zero level.

Altitude calibrations of microphones B and C obtained with an electrostatic actuator (ref. 6) are also presented in figure 3. Altitude calibrations were not obtained for microphone A because data supplied by the manufacturer indicated negligible effect of altitude on this microphone, except at its resonant frequency (approximately 11,000 cps). Therefore, a cutoff filter was used in reducing the data to compensate for the resonant frequency.

The laboratory calibrations of the microphones and the electrical calibration of the data-recording and reduction system were combined to obtain the total response of the data-acquisition system (figs. 4(a) to 4(c)).

Microphones respond to variations from the average pressure; this response varies with the angle of impingement of the pressure fluctuations on the face of the microphone. The pressure variations in the boundary layer are assumed to propagate parallel to the face of the microphone. The Bureau of Standards calibration of microphone A would, therefore, be the correct calibration. The angle of impingement on the face of microphone B at station 10 and on the face of microphone C was assumed to be random, and the angle of impingement on the face of microphone B in the acoustic isolation chamber was assumed to be perpendicular. The data obtained with microphones B and C were corrected for angle of impingement by using the corrections presented in reference 7.

ACCURACY

Table I presents the octave-band corrections for microphones A, B, and C. These corrections are based on the assumption of white noise, and include data recording and playback response, filter characteristics, effect of altitude, and angle of impingement of the pressure variations on the microphones. By applying the corrections, a variation of ± 1.5 decibels or less was indicated for the mean overall uncorrected levels for microphones A and B at a given altitude over the dynamic-pressure range of the data. The calibration of the microphones and the assumptions on which the calibrations are based give an accuracy of ± 1.0 decibel. Therefore, the absolute levels of the uncorrected mean overall levels have an accuracy of ± 3 decibels for microphones A and B. Microphone C had an absolute error up to 7 decibels.

TESTS

The data were obtained at altitudes of about 26,000 feet and 40,000 feet to determine the effect of Mach number and dynamic pressure. The Mach number range was from approximately 0.8 to 2, and the dynamic pressure ranged from approximately 200 lb/sq ft to 1,000 lb/sq ft. The data were obtained during relatively stable atmospheric conditions. A wire was installed around the cone 2.25 inches from the apex for one flight to trip the boundary layer and assure a turbulent boundary layer over most of the cone surface.

Three flight techniques were used: (1) Most of the data were obtained during acceleration at full military power and deceleration at reduced power. From these tests it was possible to show that engine noise was not an important contribution to the measured noise. (2) Stable-flight conditions (constant Mach number, engine power, and altitude) were established to ascertain that acceleration did not affect

the measurements. (3) Noise levels were recorded during a steady turn to determine the effect of angle of attack.

RESULTS AND DISCUSSION

The results of this investigation are presented as the variation of the overall mean noise level with dynamic pressure; the variation of free-stream Mach number and Mach number in the boundary layer with dynamic pressure; the variation of the noise levels with time, for two flight conditions with constant dynamic pressures, to show effects of angle of attack; and the faired maximum and minimum overall noise levels and the noise levels in various octave bands at selected dynamic pressures for each of the microphone locations.

F
1
6
C

Overall Noise Levels

Figures 5(a) to 5(d) present the variation of the measured mean overall noise levels with free-stream dynamic pressure during accelerations and decelerations. The overall measured levels of microphones A and B are accurate to ± 3 decibels. Corrections for frequency distribution give a relative error of ± 1.5 decibels for microphones A and B at a given altitude for the dynamic-pressure range of the tests. Microphone C has an overall measured level error of 7 decibels at a dynamic pressure of 1,000 lb/sq ft. Corrections for frequency distribution of the pressures measured at microphone C to obtain the relative error at a given altitude would lower the overall levels approximately 1 decibel at a dynamic pressure of 300 lb/sq ft and approximately 5.5 decibels at a dynamic pressure of 1,000 lb/sq ft.

The boundary-layer microphone and internal microphone show a definite increase in noise level with an increase in dynamic pressure (figs. 5(a) and 5(b)). Intermittent changes were observed in the boundary-layer-noise level obtained for the smooth cone at $h_p \approx 40,000$ feet (fig. 5(a)). Additional data not presented showed that the large change in the boundary-layer noise for the smooth cone at $h_p \approx 40,000$ feet occurred over a range of $M \approx 1.2$ to $M \approx 2.0$ during various flights. These large changes were not a momentary transient, but often continued for a change in Mach number as large as 0.2. Therefore, it would appear that the changes in boundary-layer-noise level were not caused by shock waves. These changes did not occur at $h_p \approx 26,000$ feet or after the installation of a trip wire for the tests at $h_p \approx 40,000$ feet. Except for the large variations for the smooth

cone at $h_p \approx 40,000$ feet, any effect of altitude was indefinite because of calibration accuracies obtainable.

The boundary-layer-noise level was assumed to vary radially and longitudinally on the surface of the cone, and the large changes in the boundary-layer-noise levels were assumed to be localized in the boundary layer in the vicinity of microphone A at the time they were measured and at other locations on the cone at other times. These assumptions are necessary to explain why the large changes in boundary-layer-noise level (fig. 5(a)) did not cause large changes in the internal-noise levels measured, at the same time, at stations 10 and 55 (figs. 5(b) and 5(c)). The internal microphones respond to the noise transmitted through the surface of the cone over the microphone compartment. No attempt was made to obtain the acoustic attenuation of noise through the wall of the cone, since the distribution of noise around the cone was not believed to be symmetrical.

The variation of free-stream Mach number and the local Mach number at the boundary-layer-noise measuring position for several distances from the surface of the cone are presented in figure 6. The boundary layer for the smooth cone at $h_p \approx 40,000$ feet (fig. 6(a)) shows a decided change in the variation of local Mach number with free-stream dynamic pressure for $q \approx 500$ lb/sq ft. No changes of such magnitude for the local Mach number are evident for the cone with the trip wire at $h_p \approx 40,000$ feet (fig. 6(b)) or for the smooth cone at $h_p \approx 26,000$ feet (fig. 6(c)). It should be noted that the boundary-layer-rake measurements and the noise measurements were made on different flights. Therefore, it is assumed that the large variations in local Mach number occurred at different free-stream Mach numbers on different flights and were the result of varying turbulence level in the boundary layer.

Unpublished measurements of overall internal-noise levels for this cone, obtained in a wind tunnel for stations 10 and 49, differed from the flight results. The wind-tunnel internal-noise-level data were obtained with Shure 98-98 microphones and a sound-level meter. Steady-state flow conditions in the tunnel resulted in considerable fluctuations in the overall sound-level reading and necessitated the operator's interpretation of the levels. Wind-tunnel data indicated a higher noise level at station 10 than was obtained in flight. When acoustic isolators were placed in the vents during the wind-tunnel tests, the levels at station 49 were lower than obtained in flight, but without the isolators the levels at station 49 were higher. The wind-tunnel results indicate that the vent used on the cone in flight affected the internal-noise levels at station 55.

The internal microphones at station 10 or station 55 and the microphone in the acoustic isolation chamber at station 55 (figs. 5(b) to 5(d)) generally showed an increase in noise level at dynamic pressures in the transonic range ($q < 600$ lb/sq ft), then a decrease in noise level with a limited increase in dynamic pressure. This variation, which appears to be a Mach number effect, was greater than relative measuring accuracy and was more pronounced at $h_p \approx 26,000$ feet than at $h_p \approx 40,000$ feet.

Figure 7 presents time histories of measured boundary-layer-noise levels, angle of attack, and free-stream dynamic pressures during stable-flight conditions and during a turn maneuver. The boundary-layer-noise levels were essentially constant during the turn ($M \approx 1.2$, $h_p \approx 40,000$ ft)

where the measured angle of attack varied from approximately 1° to 5° . Large variation in the boundary-layer-noise level was present during the stable-flight conditions ($M \approx 1.4$, $h_p \approx 40,000$ ft) where the angle of

attack was less than 1° . The large variations in boundary-layer-noise levels shown in figure 5(a) also occurred at an angle of attack of approximately 0° . Other flight data not presented showed this same variation. Small variations in angle of attack or angle of yaw near 0° could cause changes in turbulence level at the boundary-layer-noise-level measuring station.

Noise-Pressure Spectra

Figures 8 to 11 present the octave-band pressure spectra at selected dynamic pressures for the four microphone positions in the nose cone. The corrections shown in table I were made to the data, and the overall levels were determined by summing mean noise levels in the corrected octave bands. The magnitudes of the level variations are the measured variation of level.

The octave-band noise-pressure levels for all microphone positions generally showed larger deviation in level for the octave bands below 2,400 cps than for the higher octave bands because of the larger number of frequencies in the higher band. The large variations in level at the lower frequencies indicate that estimation of structural-fatigue life on the basis of the average level could lead to serious error. Installation of a trip wire did not change the frequency distribution by an appreciable amount except for the boundary-layer microphone where $q = 600$ lb/sq ft at an altitude of 40,000 feet. The overall noise levels for the boundary layer and the internal microphone at station 55 had variations of 5 decibels or less (figs. 8(a) to 8(d) and 9(a) to 9(d)), except for the boundary-layer microphone at $q = 600$ lb/sq ft where large variations were noted previously in figure 5(a). The noise levels at station 10 and in the acoustic isolation chamber at station 55

(figs. 10(a) to 10(d) and 11(a) to 11(d)) had larger variations in the overall noise level than the internal levels at station 55.

The octave-band noise levels in the boundary layer at station 55 for the smooth cone at $h_p \approx 40,000$ feet and a dynamic pressure of 600 lb/sq ft (fig. 8(b)) show a large increase for octave bands below 2,400 cps. The large increase in the octave-band noise levels is reflected in the large increase in overall level. The lack of increase in the octave-band noise level above 2,400 cps indicated that the unsteady turbulence in the boundary layer was primarily low-frequency pressure fluctuations.

Comparison With Previous Studies

Presented in figure 12 is a comparison of boundary-layer-noise data obtained from pipe-flow experiments (ref. 3), measurements on a B-47 airplane at $h_p \approx 10,000$ feet and $h_p \approx 20,000$ feet (ref. 5), and the smooth nose cone of the present tests at $h_p \approx 26,000$ feet. The data from reference 5 and the nose-cone data are uncorrected for filter characteristics or for altitude effect. When parallel impingement is assumed on the face of the B-47 microphone, these data are accurate to approximately ± 3 decibels. As was noted previously, the uncorrected nose-cone data were accurate to ± 3 decibels for the boundary-layer station.

The pipe-flow data (ref. 3) and the data from reference 5 show reasonable agreement, but differ considerably with the nose-cone data. The pipe-flow and B-47 data varied with dynamic pressure and had a value of approximately $0.006q$. The measured nose-cone data had a value of approximately $0.001q$ at the lowest dynamic pressure at which measurements were made and approximately $0.0005q$ at the highest dynamic pressure. The pipe-flow data and the B-47 data were obtained at subsonic speeds; only the nose-cone data below $q \approx 530$ lb/sq ft at $h_p \approx 26,000$ feet were obtained at subsonic speeds. The boundary-layer thickness on the nose cone is estimated to be of approximately the same order of magnitude as the boundary-layer thickness in some of the pipe-flow experiments; whereas, minimum boundary-layer thickness of the B-47 data was several times greater. These results indicate that the difference in Mach number and boundary-layer thickness did not cause the large difference between the nose-cone data and the pipe-flow and B-47 data. It should be noted that estimating the boundary-layer noise on the basis of $0.006q$ determined for subsonic flows would be conservative for forward surfaces of a body and may be a reasonable approximation for surfaces farther rearward on the body except in regions of separated flow or in the wake of protuberances.

CONCLUSIONS

In-flight measurements of the noise environment of a Fiberglas nose cone indicated that:

1. The measured overall noise levels on the surface of the nose cone increased with increasing dynamic pressure. The average sound-pressure level varied from approximately 0.001 of the lower dynamic pressures to 0.0005 of the higher dynamic pressures, instead of 0.006 of the dynamic pressure determined in previous studies.

2. Variations in angle of attack of approximately 1° to 5° had negligible effect on aerodynamic-noise levels for an included-angle cone of 24.5° . At angles of attack near 0° , large variations in the noise levels on the surface of the cone at an altitude of 40,000 feet were attributed to variations in turbulence level.

H
1
6
0

3. Large variations in aerodynamic-noise level occurred at frequencies less than 2,400 cycles per second. These variations result in serious error in structural-fatigue life when the average level is used for such tests.

Flight Research Center,
National Aeronautics and Space Administration,
Edwards, Calif., January 17, 1962

REFERENCES

1. Curle, N.: The Influence of Solid Boundaries Upon Aerodynamic Sound. A.R.C. 17,373, F.M. 2188, British Aero. Res. Council, Feb. 5, 1955.
2. Phillips, O. M.: On Aerodynamic Surface Sound. A.R.C. 16,963, F.M. 2099 (rev.), British Aero. Res. Council, March 28, 1955.
3. Willmarth, W. W.: Space-Time Correlations and Spectra of Wall Pressure in a Turbulent Boundary Layer. NASA Memo 3-17-59W, 1959.
4. Mull, Harold R., and Algranti, Joseph S.: Preliminary Flight Survey of Aerodynamic Noise on an Airplane Wing. NACA RM E55K07, 1956.
5. McLeod, Norman J., and Jordan, Gareth H.: Preliminary Flight Survey of Fuselage and Boundary-Layer Sound-Pressure Levels. NACA RM H58B11, 1958.
6. Beranek, Leo L.: Acoustic Measurements. John Wiley & Sons, Inc., c. 1949, pp. 173-176.
7. Vaneklasen, Paul S.: Instrumentation for the Measurement of Sound Pressure Level With the Western Electric 640AA Condenser Microphone. Jour. Acoustical Soc. of Am., vol. 20, no. 6, Nov. 1948, pp. 807-817.

TABLE I.- OCTAVE-BAND CORRECTIONS FOR NOSE-CONE DATA

Octave band, cps	Corrections, decibels							
	Microphone A	Microphone B				Microphone C		
		Cone station 10		Acoustic isolation chamber, station 55				
		$h_p \approx 26,000$ ft	$h_p \approx 40,000$ ft	$h_p \approx 26,000$ ft	$h_p \approx 40,000$ ft	$h_p \approx 26,000$ ft	$h_p \approx 40,000$ ft	$h_p \approx 26,000$ ft
20 to 75	1.0	0	0	0	0	-0.5	0	0
75 to 150	-.5	-0.5	-1.0	-0.5	-0.5	-1.0	-1.0	-1.0
150 to 300	-1.0	-.5	-1.0	-.5	0	-1.0	-1.0	-1.0
300 to 600	-1.5	-1.0	-1.5	-1.0	-1.5	-1.5	-1.5	-1.5
600 to 1,200	-.5	-1.0	-1.5	-.5	-1.5	-1.5	-1.5	-1.5
1,200 to 2,400	1.0	0	-.5	-1.0	-1.0	-.5	-.5	-.5
2,400 to 4,800	-.5	-1.5	-1.5	-4.0	-4.0	-2.5	-2.5	-2.5
4,800 to 10,000	1.0	-6.0	-7.5	-10.5	-12.0	-7.0	-9.0	-9.0

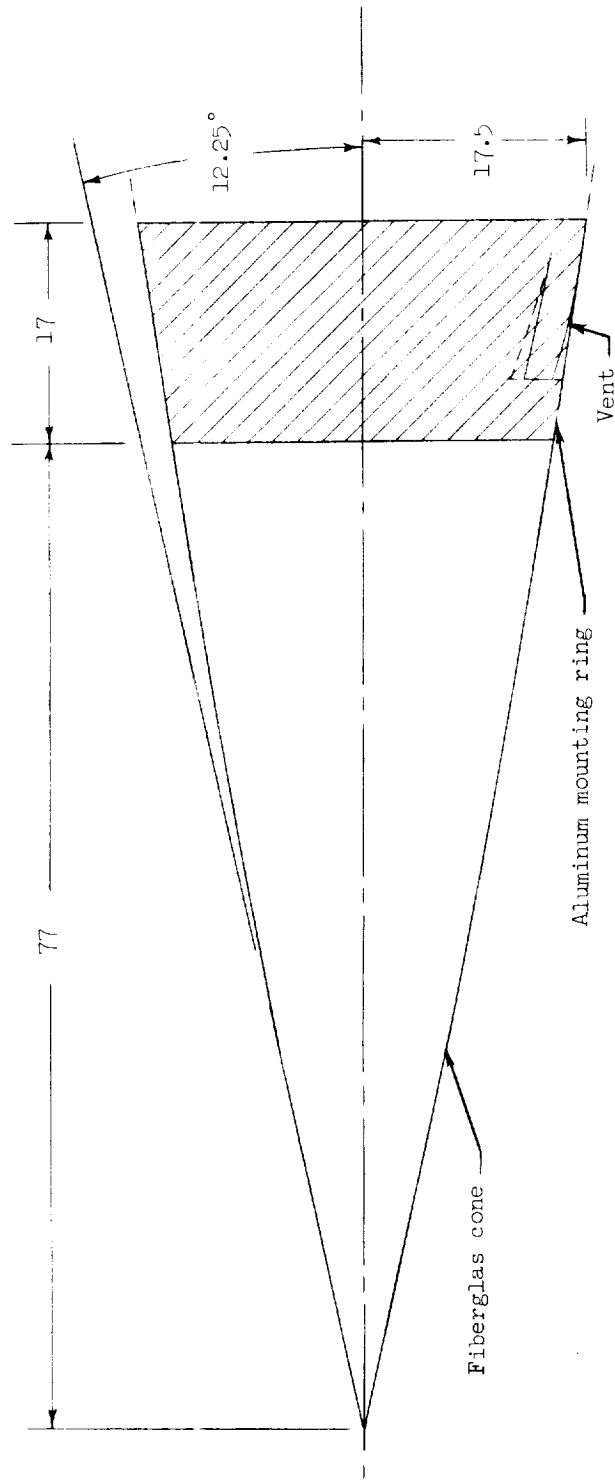
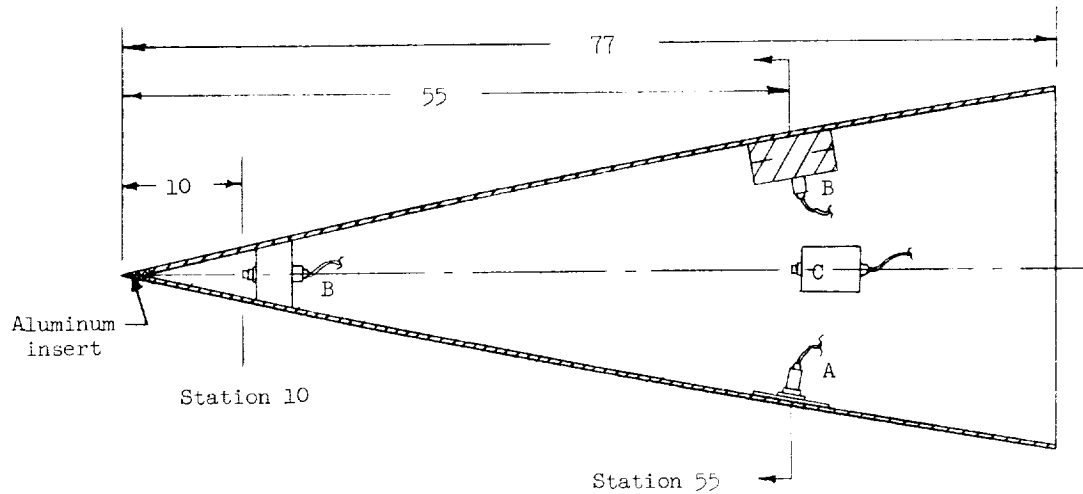
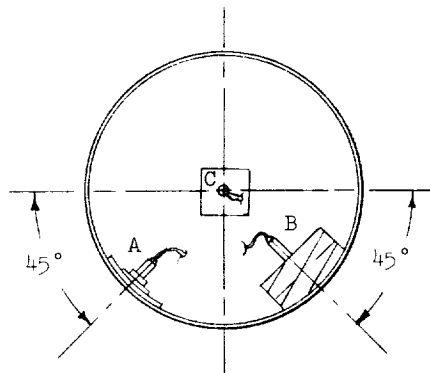


Figure 1.- Sketch of Fiberglas nose cone and aluminum mounting ring. All dimensions in inches unless otherwise noted.



(a) Schematic longitudinal position of microphones.



(b) Radial position of microphones at station 55 viewed from base of cone.

Figure 2.- Sketch of microphone locations in nose cone. All dimensions in inches unless otherwise noted.

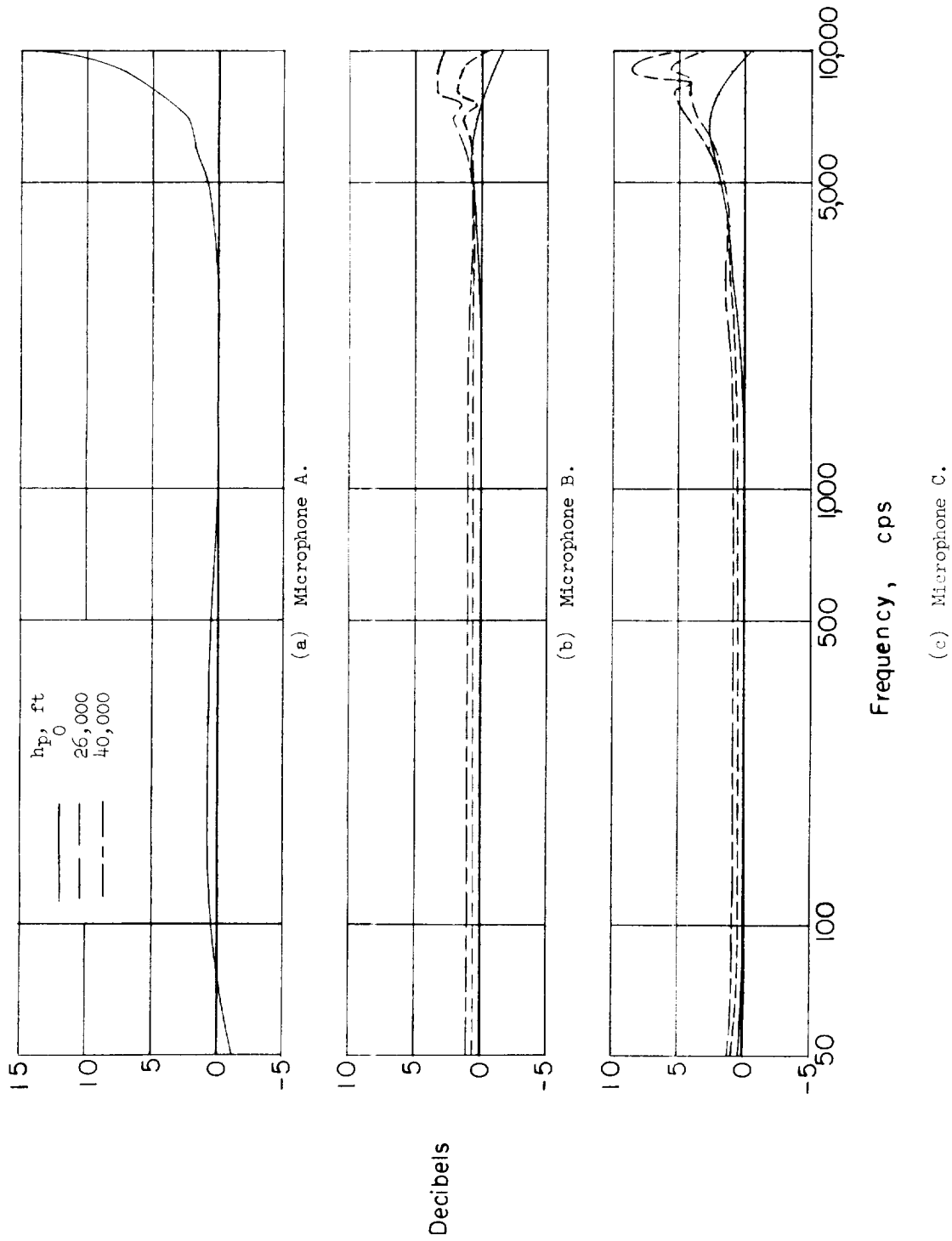


Figure 3.- Microphone calibrations.

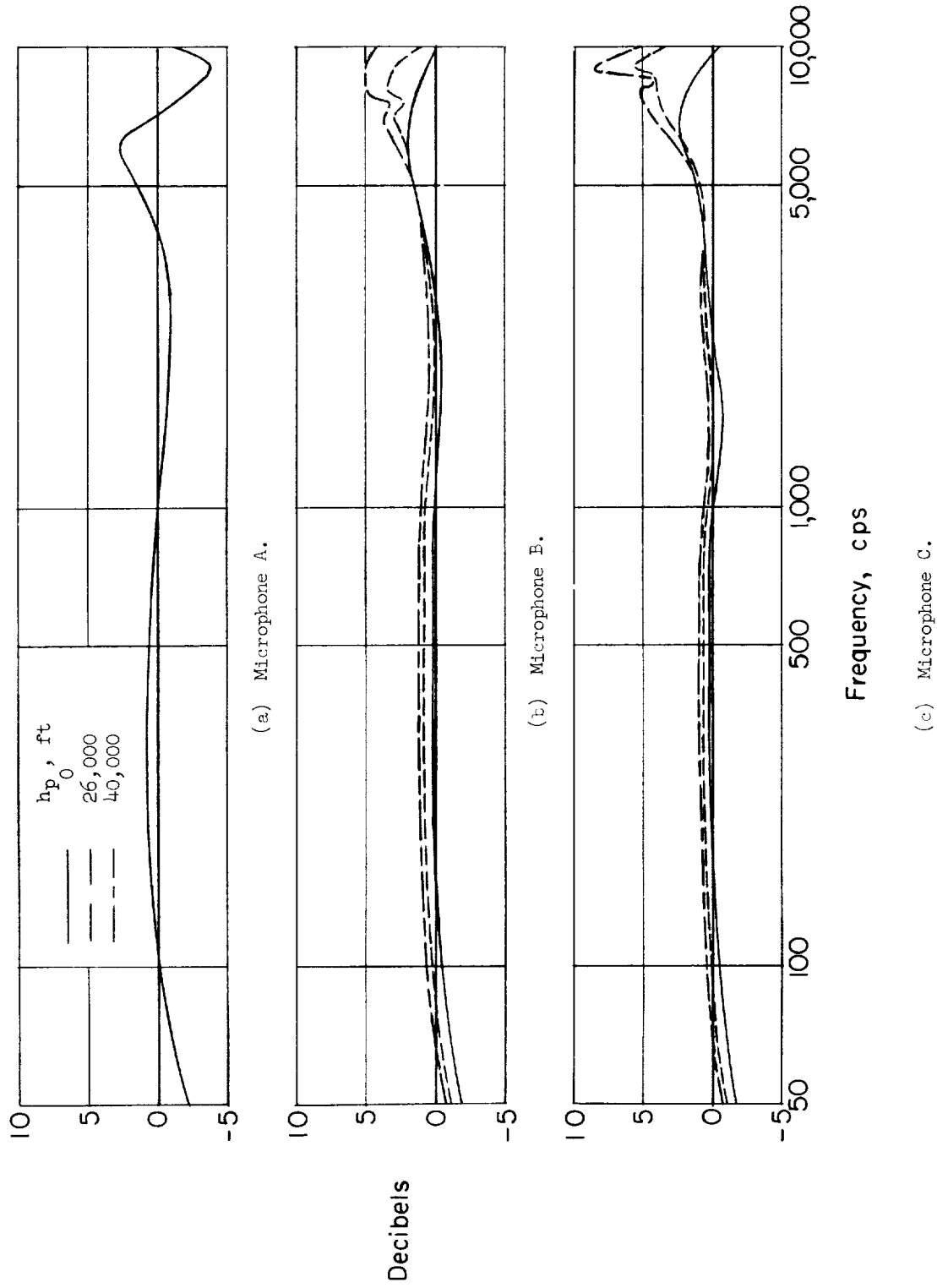


Figure 4.- Combined frequency response of microphone and data-recording and reduction system.

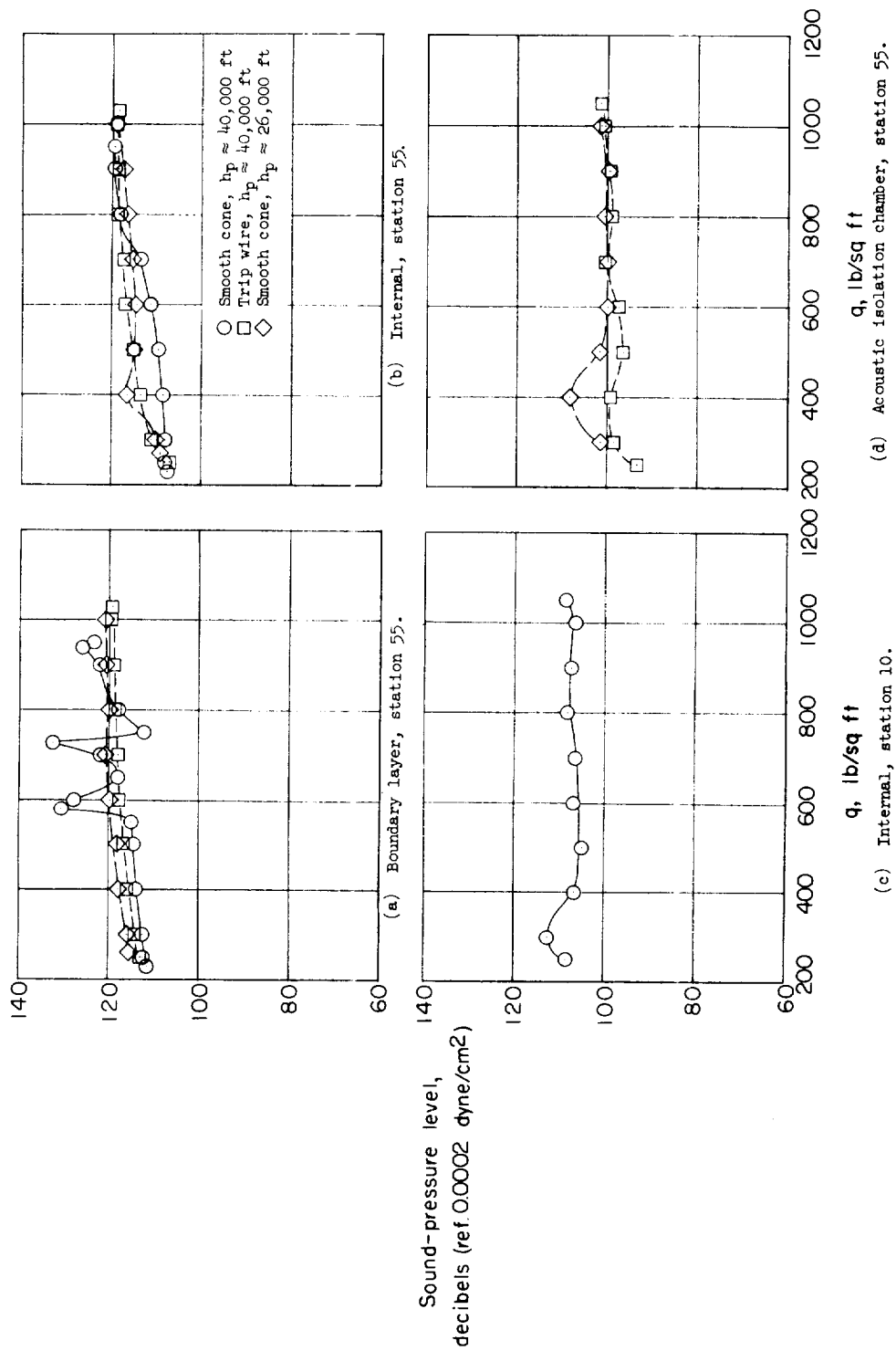


Figure 5.- Variation of mean overall noise level with airplane free-stream dynamic pressure.

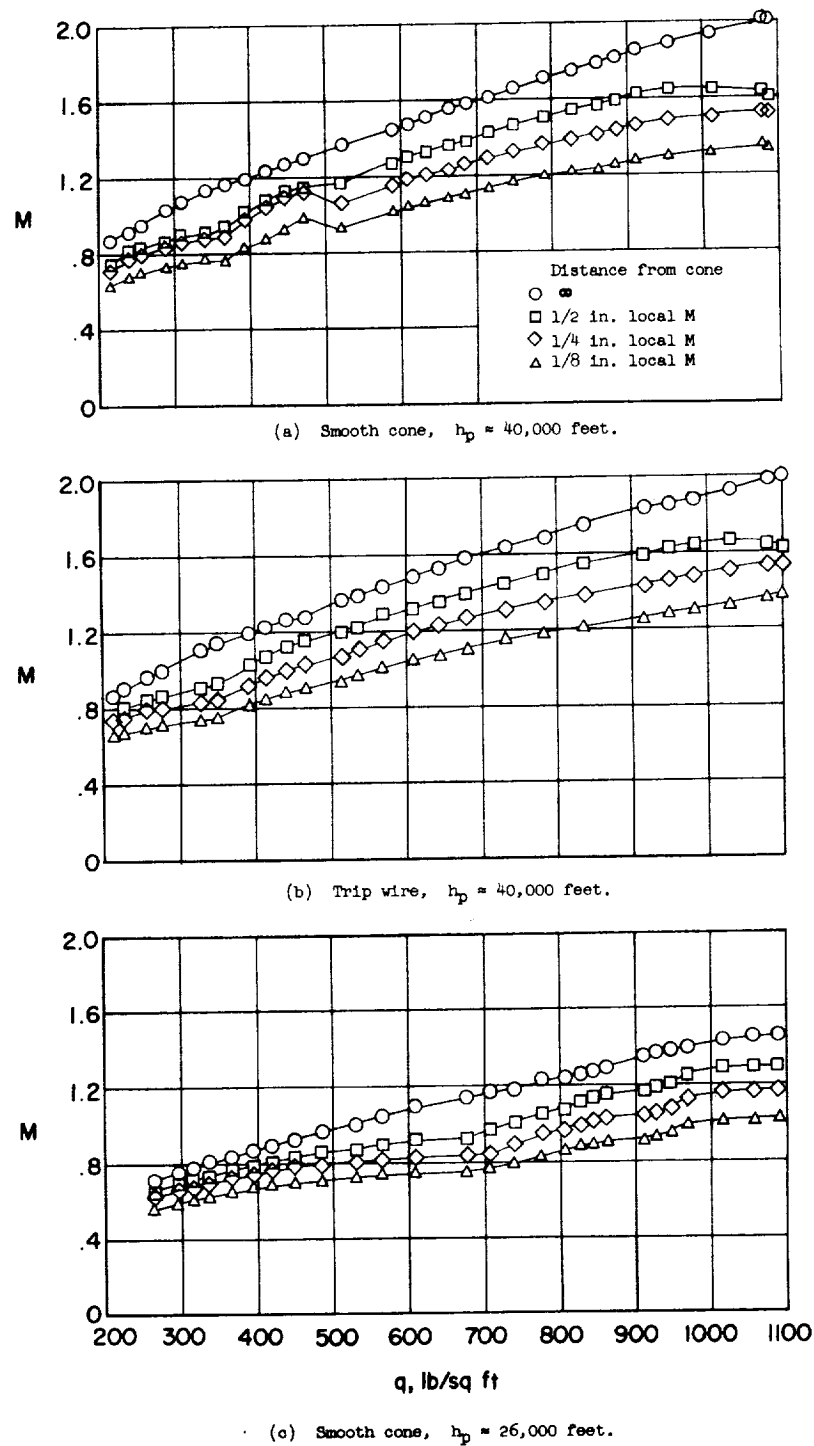


Figure 6.- Variation of free-stream and local Mach number with free-stream dynamic pressure at station 55.

H-160

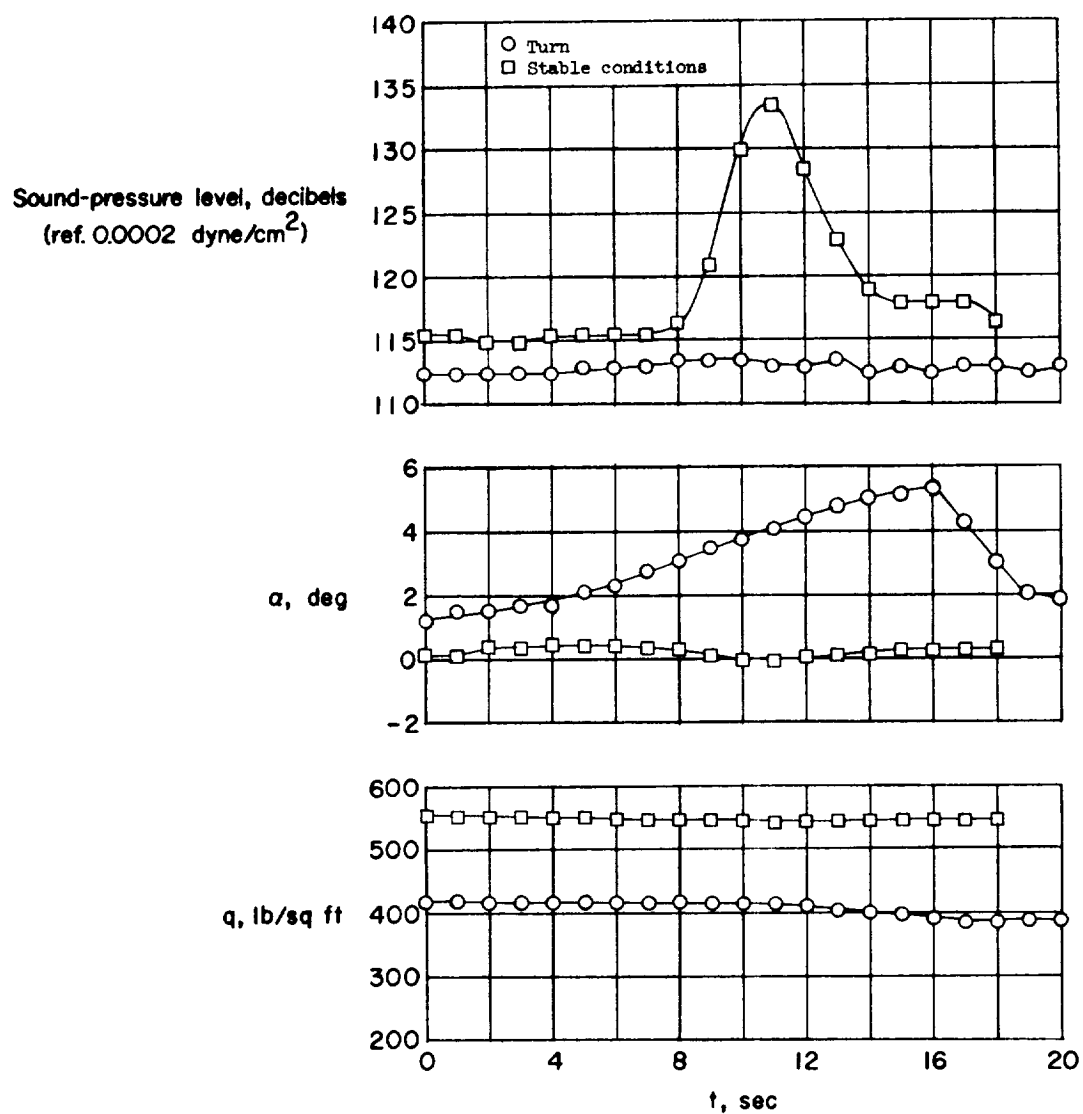


Figure 7.- Effect of angle of attack on boundary-layer noise levels.
 $h_p \approx 40,000$ feet.

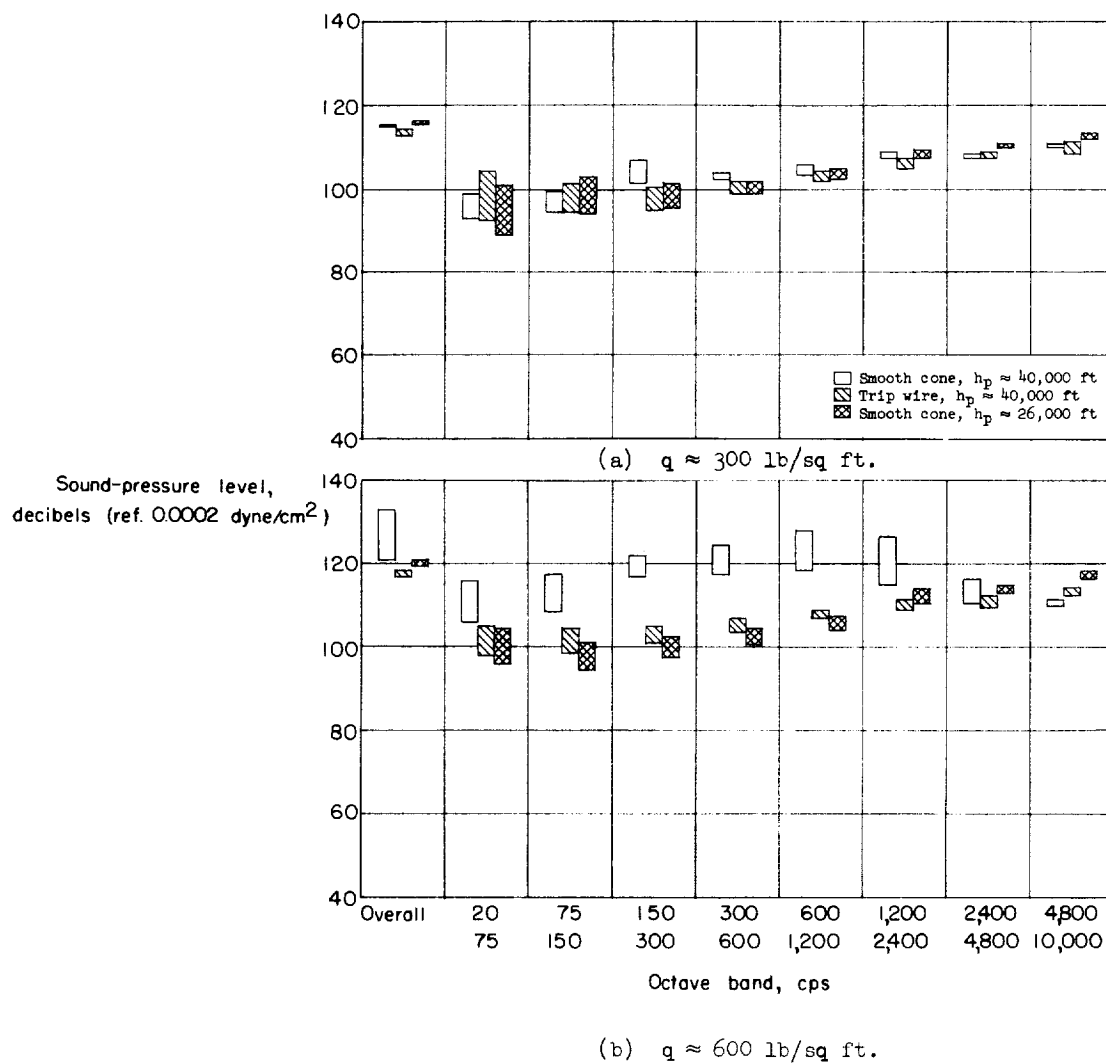


Figure 8.- Noise pressure spectra and magnitude of pressure variation at various airplane free-stream dynamic pressures at boundary-layer station 55.

H-160

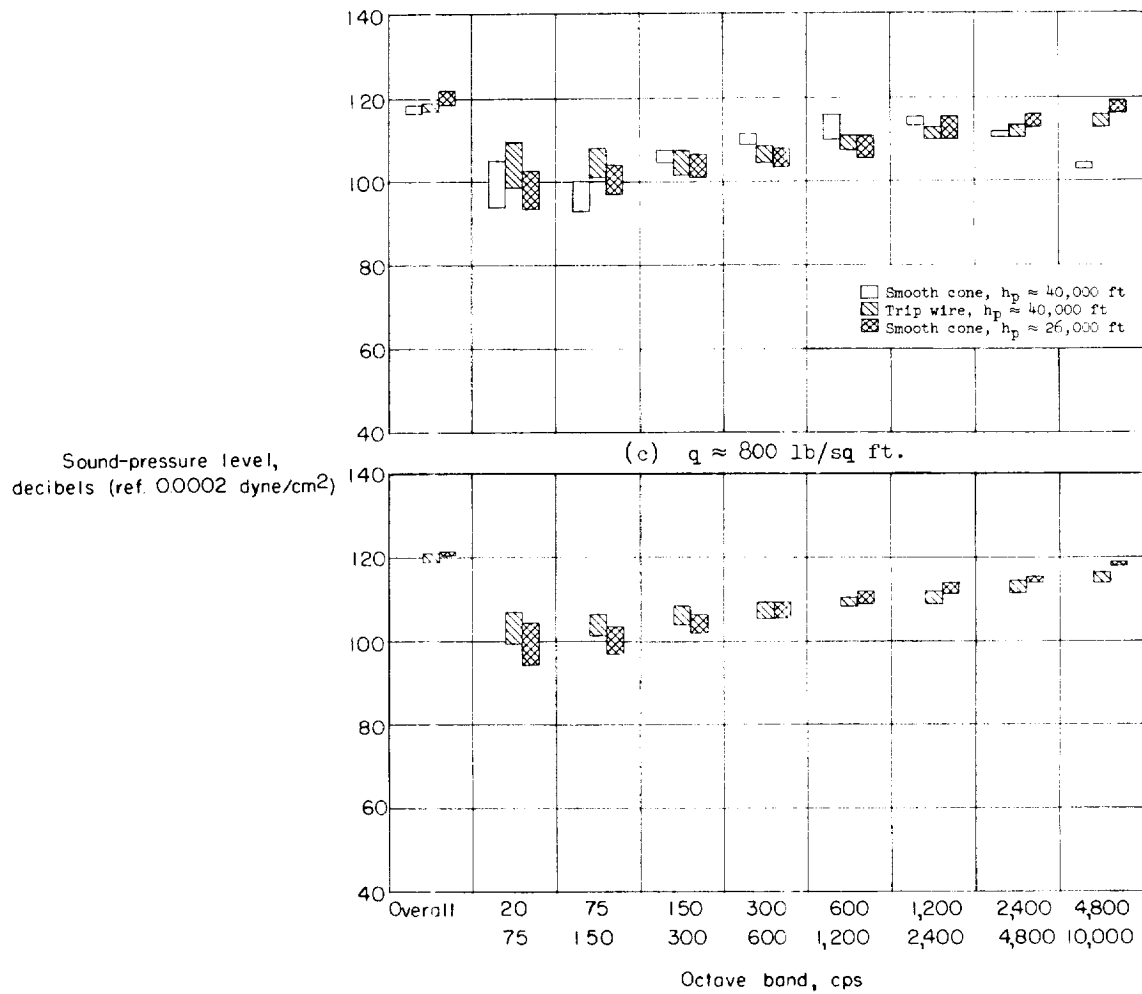


Figure 8.- Concluded.

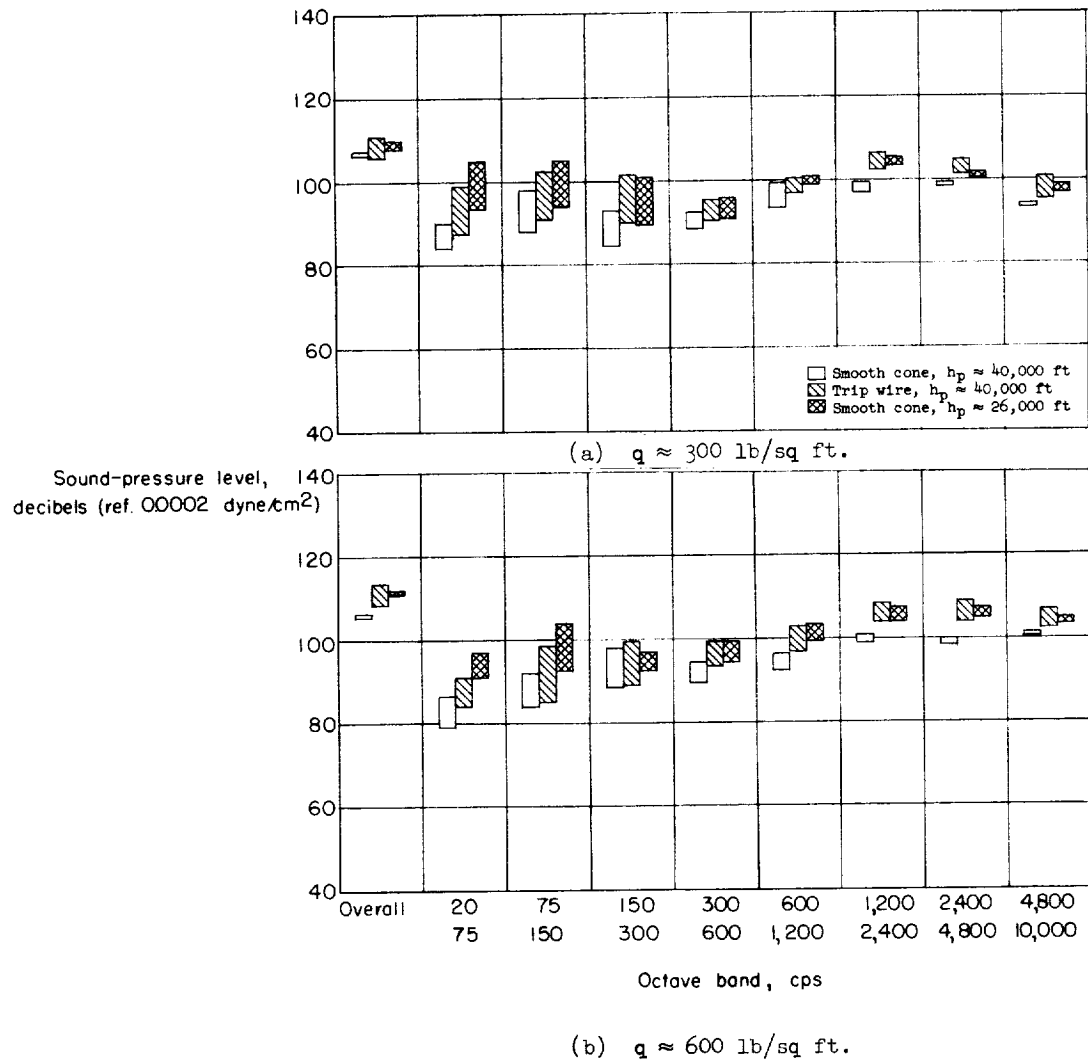


Figure 9.- Noise pressure spectra and magnitude of pressure variation at various airplane free-stream dynamic pressures at internal station 55.

H-160

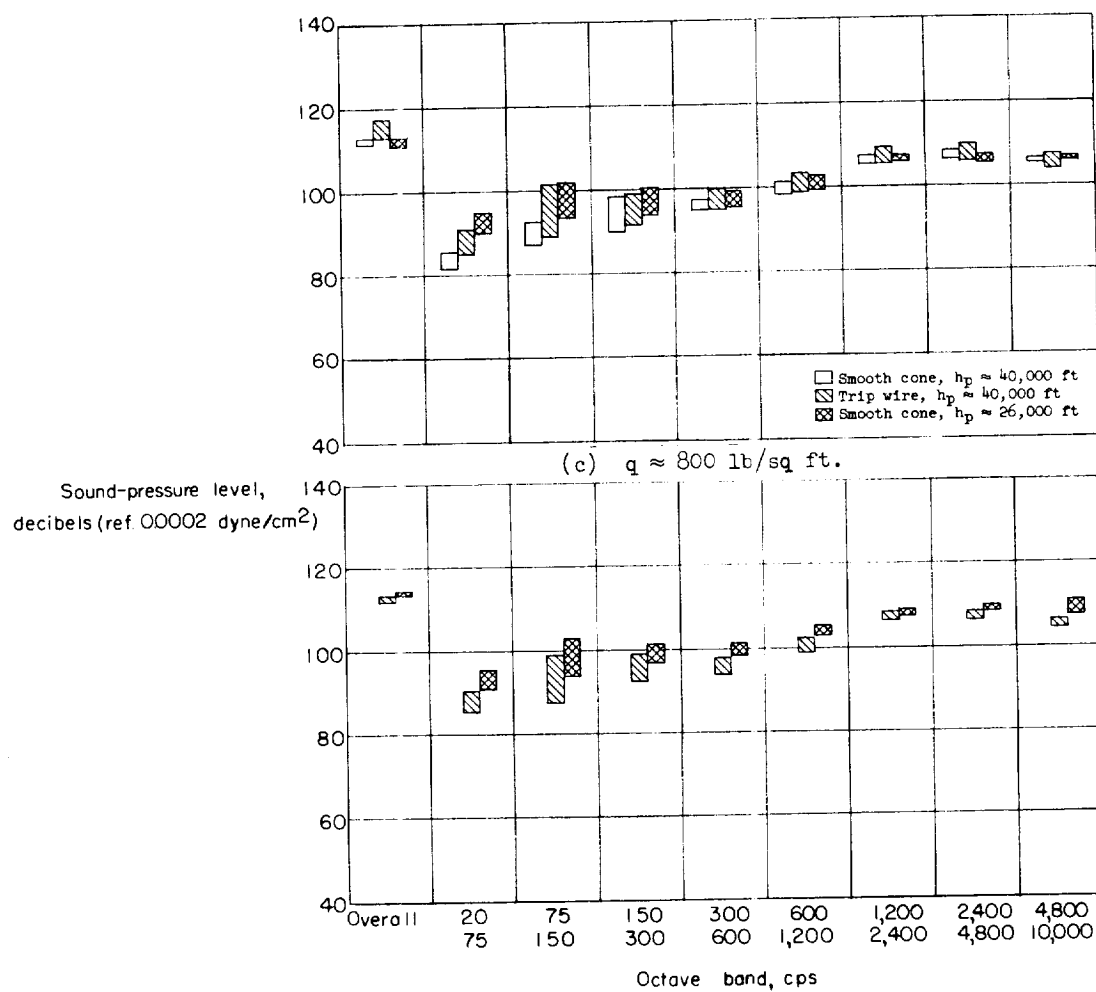


Figure 9.- Concluded.

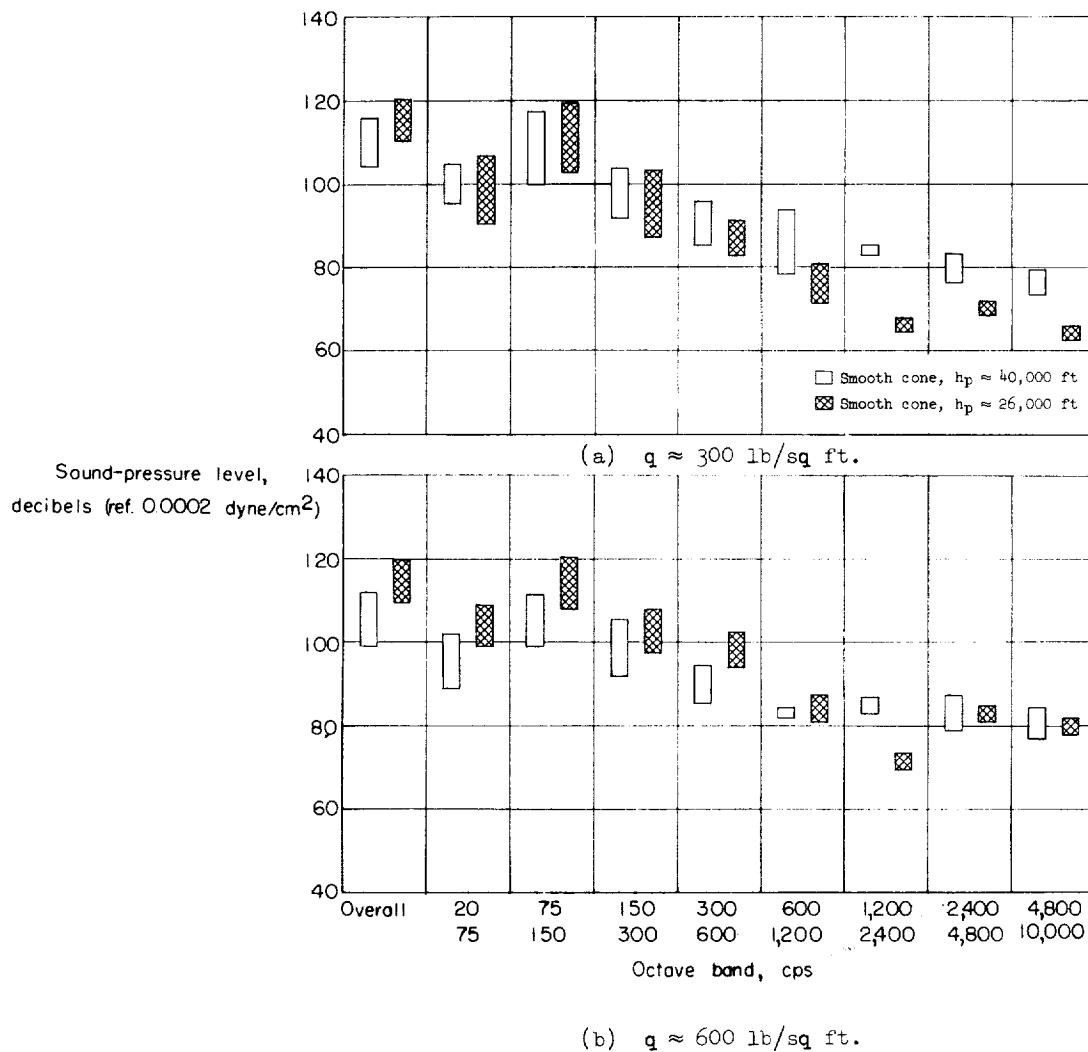


Figure 10.- Noise pressure spectra and magnitude of pressure variation at various airplane free-stream dynamic pressures at internal station 10.

H-160

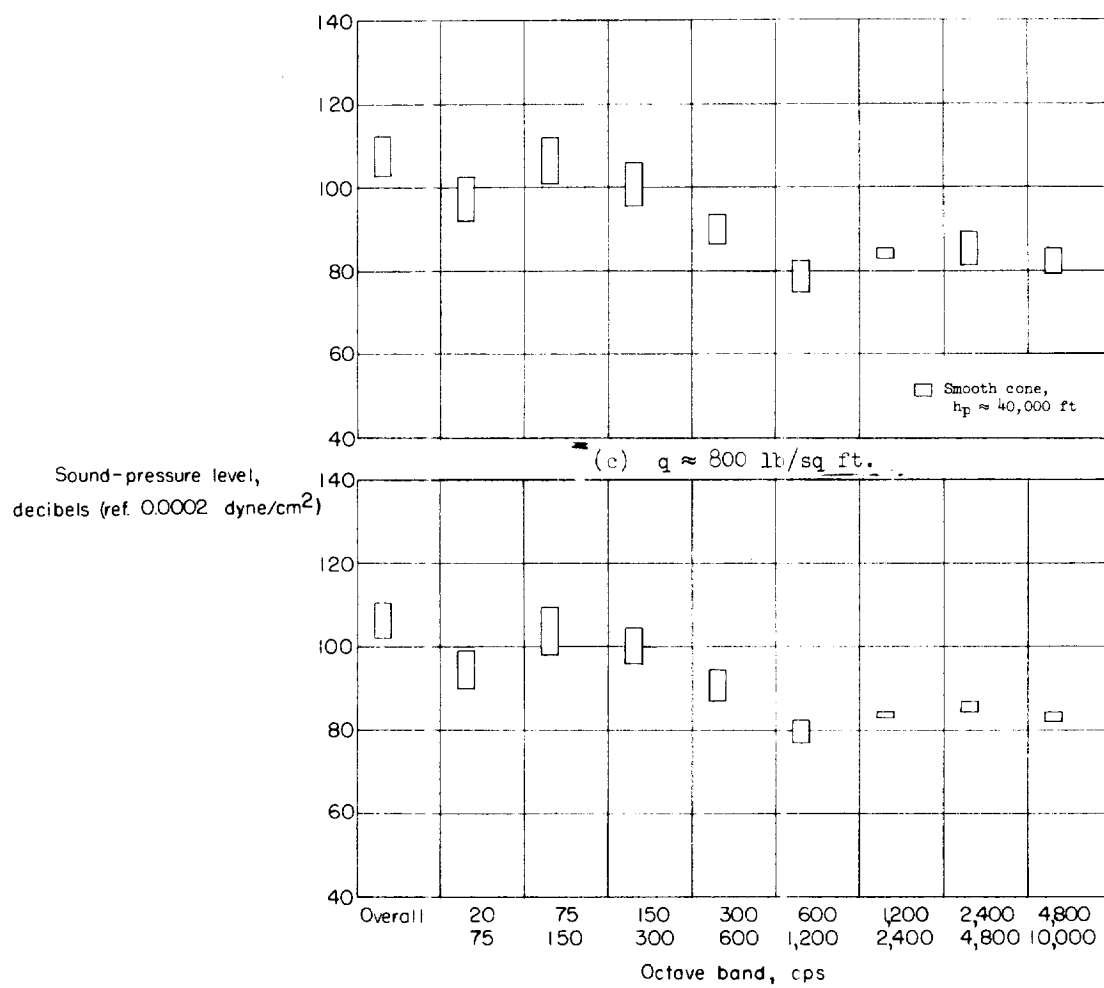


Figure 10.- Concluded.

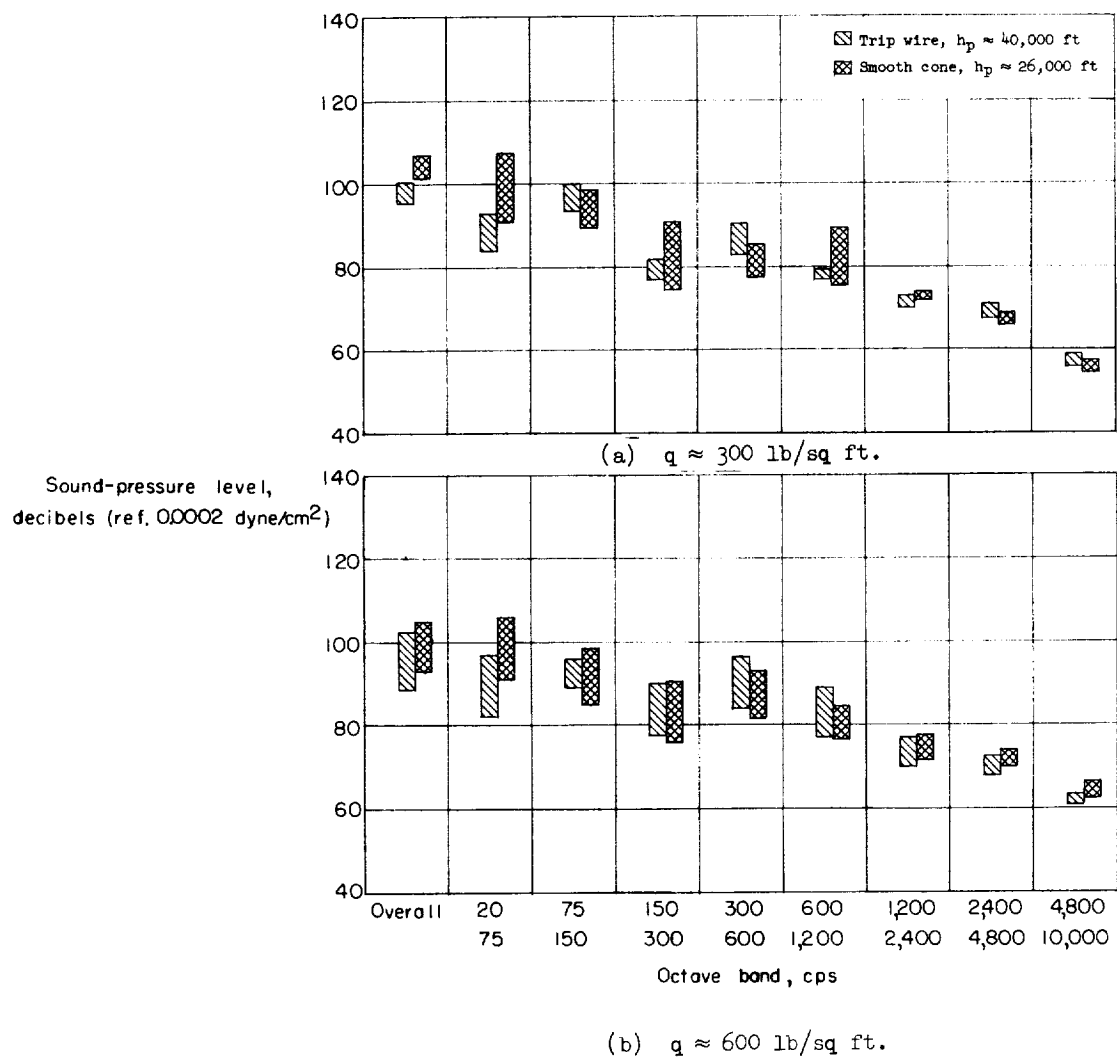


Figure 11.- Noise pressure spectra and magnitude of pressure variation at various airplane free-stream dynamic pressures. Acoustic isolation chamber, station 55.

H-160

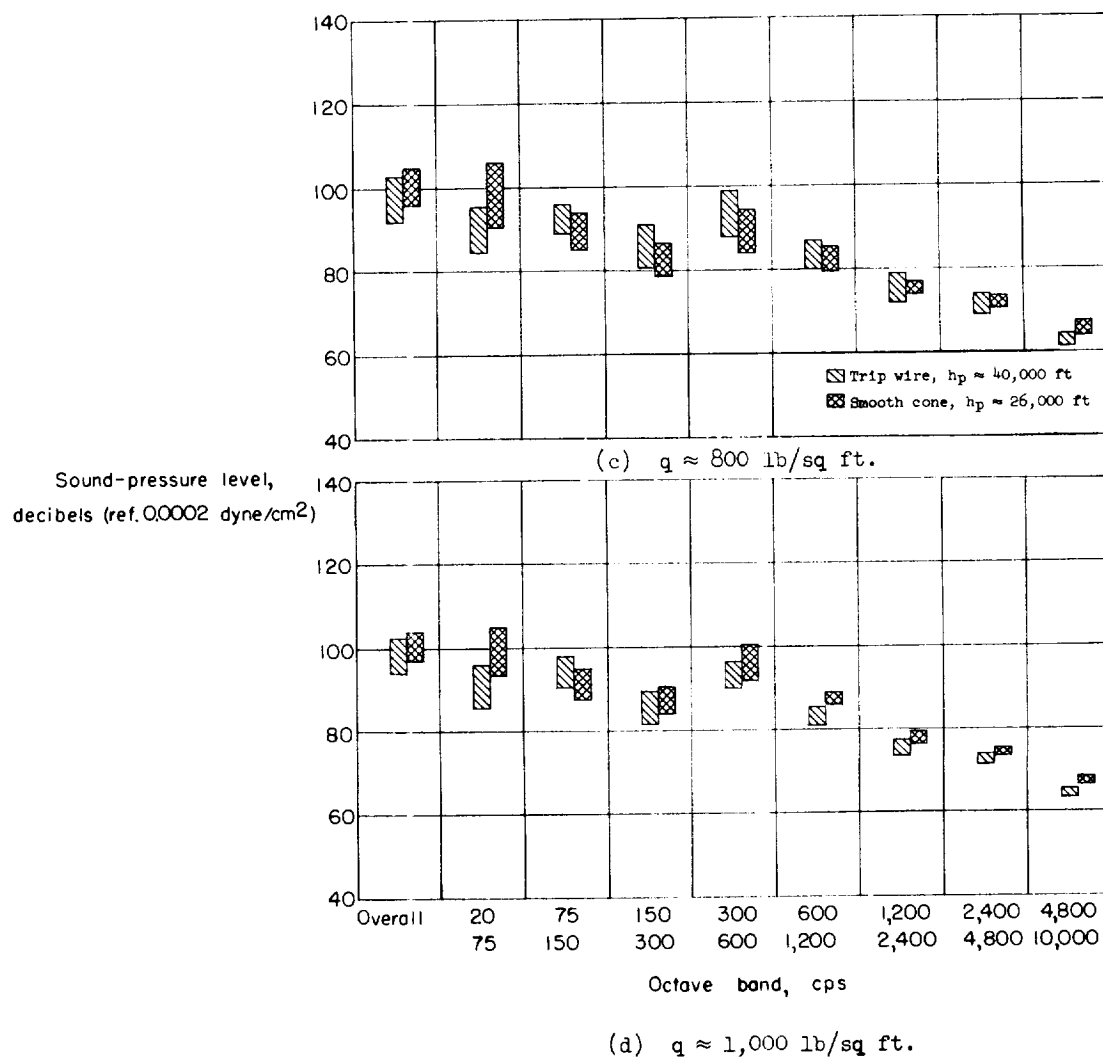


Figure 11.- Concluded.

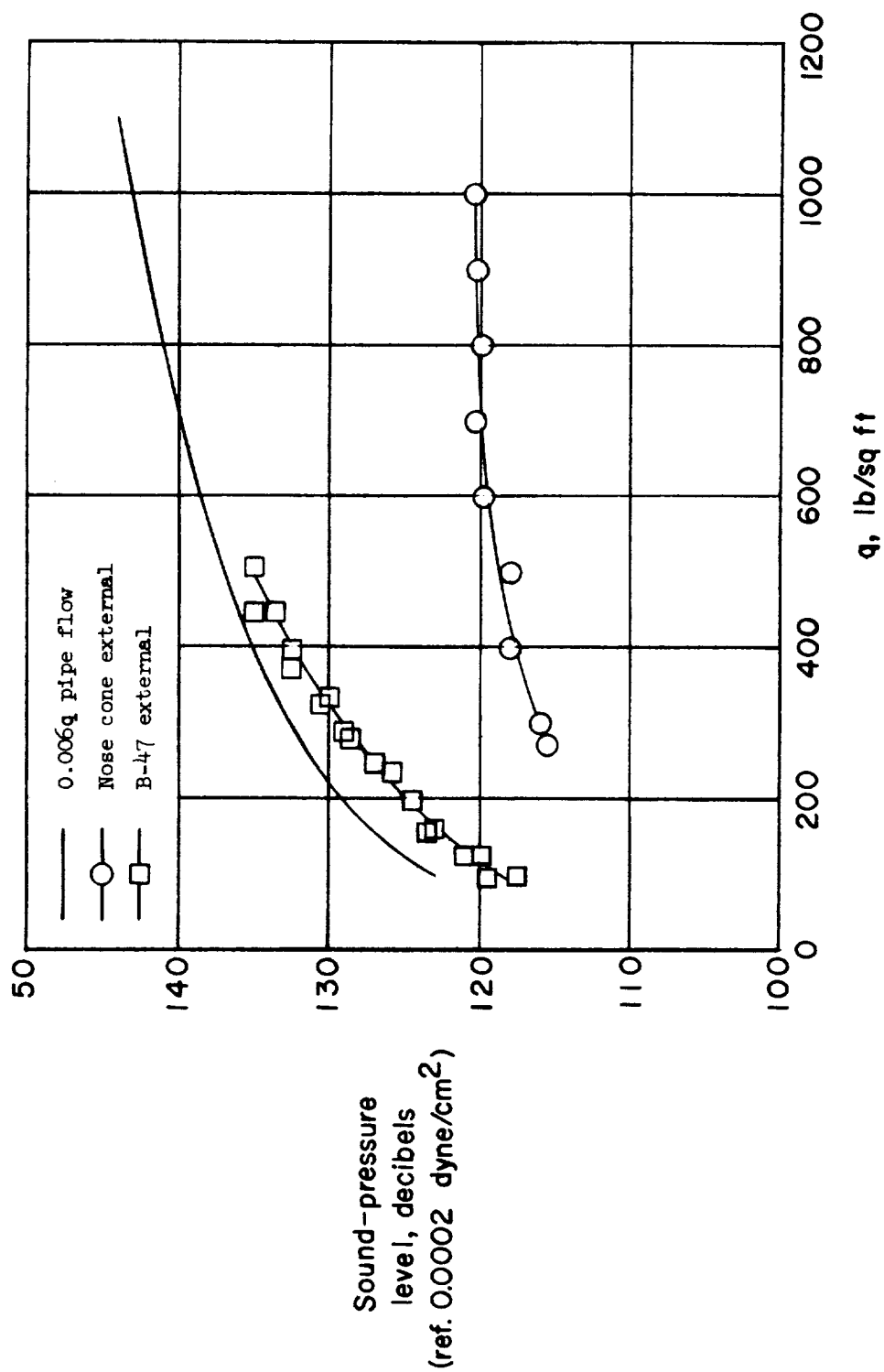


Figure 12.- Comparison of boundary-layer noise from pipe-flow, B-47, and nose-cone data.